Spatially selective laser cooling of carriers in semiconductor quantum wells

Danhong Huang, T. Apostolova, P. M. Alsing, and D. A. Cardimona

Air Force Research Lab, Space Vehicles Directorate, Kirtland Air Force Base, New Mexico 87117, USA

A successive four-step model is proposed for spatially selective laser cooling of carriers in undoped semiconductor quantum wells. The four physical steps include the following processes: (1) cold electrons with nearly zero kinetic energy are initially excited across a bandgap in a coherent and resonant way by using a weak laser field; (2) the induced cold carriers in two different bands are heated via inelastic phonon scattering to higher-energy states above their chemical potentials; (3) the resulting hot electrons and holes radiatively recombine to release photons, thus extracting more power from the quantum well than that acquired during the weak pump process; and (4) hot phonons in two surrounding hot barrier regions thermally diffuse into the central cool quantum well, thereby cooling the entire lattice with time. Based on this model, a thermal-diffusion equation for phonons including source terms from the carrier-phonon inelastic scattering and the thermal radiation received by the lattice from the surrounding environment is derived to study the evolution of the lattice temperature. At the same time, an energy-balance equation is applied to adiabatically find the spatial dependence of the carrier temperature for a given lattice temperature at each moment. There are two interesting findings in this paper. First, a V-shape feature in the carrier temperature is predicted by numerical calculations, which becomes apparent only for initial lattice temperature above 150 K. Second, a thermal-drag of the carrier temperature is found as a result of the strong carrier-phonon scattering. The difference between the lattice and carrier temperatures resulting from the thermal-drag effect is larger in the barrier regions than in the well region.

I. INTRODUCTION

Semiconductor quantum-well infrared photodetectors generally need to be cooled in order to work more efficiently.[1] Carrier cooling in quantum-well photodetectors will directly lead to a reduction of noise and an enhancement of device detectivity. There have been two different approaches to cooling quantum wells, namely the direct and indirect approaches. The direct approaches known to us include resonant tunneling,[2] nonresonant thermionic cooling,[25] and tunnel-junction cooling.[4] The indirect approaches, on the other hand, include optothermionic cooling,[5] thermoelectric cooling,[6] and fluorescent cooling.[7] Some of the above cooling concepts provide very attractive possibilities for cryogenics on a chip, either including contacts for a current flow under a bias or excluding contacts by replacing the bias with a resonant optical field. Optical on-chip cooling has many advantages for space applications, such as zero vibration, no moving parts, small volume, and light weight.

The homogeneous cooling of a solid via light-induced fluorescence was proposed quite a long time ago.[8–14] In these proposals, part of the entropy due to the thermal motion of carriers in the system is carried away by fluorescent photons. Laser-induced fluorescent cooling of heavy-metal-fluoride glass doped with trivalent ytterbium ions was the first realization of this concept.[7] This was closely followed by the demonstrations of cooling in dye solutions[15] and thulium-doped glass.[16] Laser cooling of a semiconductor has recently been predicted to be able to reach much lower temperatures than cooling in glasses, however, this remains an elusive goal after having been pursued for several years.[17–21] Until recently, the only theories attempting to model the laser cooling phenomenon are local simulation theories that include

rate equations for determining the steady-state carrier density and the loss of lattice energy with several kinetic coefficients. These early theories[17,18,20] neglect the change of carrier distributions with the temperature and only apply to situations with little change of temperature. The main feature of the rate equation approach is its simplicity, but it is unable to elucidate the essential physics behind the laser-cooling phenomena. By using a nonlocal microscopic-level theory that includes the effect of carrier distributions, our previous studies of homogeneous laser cooling of bulk semiconductors have shown that the best cooling effects can be reached in wide-bandgap semiconductors under near-bandedge interband pumping by a weak field.[19] A nonlinear pumping scheme using a red laser was also proposed[21] for the homogeneous laser cooling of wide-bandgap semiconductors with an energy gap as large as 6 eV.

For the use of a wide-bandgap semiconductor, the rate for the radiative decay of photocarriers is enhanced while reducing the the reduced rate for their nonradiative decay. Therefore, the quantum efficiency of the system will be increased. Although both the rate of optical absorption and that of photoluminescence of carriers depend on the dipole moment of the carriers, the reduction of the pump-field strength will only decrease the optical absorption, but not the photoluminescence. As a result, a positive net power loss, defined as the difference between the power loss due to photoluminescence and the power gain due to optical absorption, can be reached. This positive net power loss guarantees a cooling of the system, although the speed of the temperature drop is expected to be slow due to low carrier densities and small carrier thermal energies compared to the large bandgap of the semiconductor. Here we propose a four-step microscopic model for fluorescence-induced spatially selective laser cool-
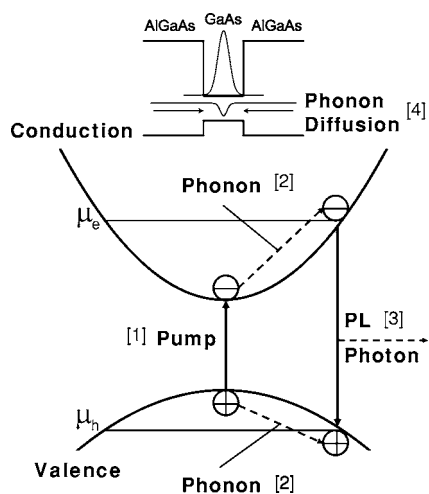
FIG. 1. An illustration of successive four steps (indicated by bracketed numbers) of photoluminescence (PL)-induced spatially selective laser cooling model for carriers in an undoped semiconductor quantum well, where $\mu_e(\mu_h)$ is the chemical potential of electrons (holes) in the quantum well. The upper inset of the figure also displays the thermal diffusion of phonons and the quantum well potential profile in the z direction, as well as the ground-state wave function of electrons (curve with a peak). The curve with a V-shape-like feature in the inset represents the spatial profile of the carrier temperature.

ing of carriers in undoped semiconductor quantum wells, which includes the change of carrier distributions with the temperature and the spatial and temporal dependence of the carrier temperature. From our numerical calculations, we have found a V-shape feature in the carrier temperature due to the quantum confinement of photocarriers and a thermal-drag of the carrier temperature due to strong carrier-phonon scattering. Most importantly, we have found that this V-shape feature becomes apparent only for high enough initial lattice temperature (above 150 K) because of the fact that the net power loss is suppressed while the lattice temperature cools down.

The organization of the paper is as follows. Section II is devoted to the establishment of our four-step selective laser cooling model and the theory for fluorescence-induced spatially selective laser cooling of carriers in undoped semiconductor quantum wells. Numerical results for the evolutions of the profile of the carrier temperatures are displayed and explained in Sec. III. The paper is briefly concluded in Sec. IV.

II. MODEL AND THEORY

In this section, we propose a microscopic theory for fluorescence-induced spatially selective laser cooling of carriers in undoped semiconductor quantum wells.[22] Our model is based on the following four successive physical steps that are graphically represented in Fig. 1. The four steps are as follows: (i) photoexcited cold carriers are initially generated near the band edges coherently by a weak laser field; (ii) the cold carriers in two bands are promoted to states above the chemical potential by phonons, thus forming Fermi-Dirac distributions; (iii) the hot electrons and holes recombine, thereby extracting heat away from the system; (iv) hot phonons thermally diffuse into the quantum well from barriers to eventually cool down the lattice and carriers of the system. This model includes the transport of phonons due to the confinement of carriers within the quantum well. It also provides us with an evolution of the spatial profile of the carrier temperature. The carriers are cooled down through thermal-drag effects.

After a dipole interaction with a weak incident pump field, cold electrons and holes are coherently produced in step one of our model, In step two, ultrafast scattering between phonons and carriers with an energy-relaxation time on the order of 0.1 to 1 ps establishes two quasiequilibrium Fermi-Dirac distributions for hot electron and hole plasmas. The detailed balance between scattering of these electron and hole plasmas gives rise to a uniform carrier temperature $T_e=T_h=T$. During this second step of our model, the carrier temperature T of the quasiequilibrium distributions depends on the instantaneous value of the lattice temperature T_L. In step three, another dipole interaction causes the hot photo-excited carriers to radiatively recombine, emitting photons that carry the combined pump plus phonon energy out of the system. In step four, the quantum confinement of carriers in a quantum well, where both the optical absorption and the photoluminescence of carriers occur, causes a spatial distribution of the lattice temperature T_L, in addition to a spatial distribution of the carrier temperature T. During the fourth step of our model, phonons from two warm barrier regions thermally diffuse into the central cool quantum well due to their finite group velocities, thereby cooling the entire lattice and cooling carriers of the system through thermal-drag effects at the same time.

To meet the criterion of laser cooling in an undoped semiconductor quantum well, the pump laser field must be weak to reduce the power gain from the absorption for the limited power loss from the photoluminescence.[19] This requirement leads to a low photocarrier sheet density n_{2D}. As a result, both the nonparabolic energy dispersion, which is important for large momentum of carriers,[23] and the exchange interaction between electrons or holes, which becomes appreciable for thermal energy k_BT of carriers below the Fermi energy,[24] can be neglected. At the same time, the weak exciton effect due to the screened exchange interaction between an electron and a hole[25] can also be ignored at moderate temperatures for AlGaAs/GaAs/AlGaAs quantum wells, since the thermal energy k_BT of carriers becomes larger than the binding energy of an exciton. In addition, the screening from the photo-excited electron and hole gases to the carrier-phonon interaction,[26] which can be described by a dielectric function of interacting carriers, will be neglected here since the correction term is expected to be proportional to n_{2D}.

The time evolution of the lattice-temperature profile $T_L(z)$ during the last step of the successive four-step selective laser cooling model is found to be determined by a thermal-diffusion equation for phonons. This equation can be directly derived from the Boltzmann transport theory with a position-dependent temperature, and is given by

$$\left\{ \sum_{\lambda} c_V^{\lambda}[T_L(z)] \right\} \frac{\partial T_{\mathrm{L}}(z)}{\partial t} = \sum_{\lambda} \frac{\partial}{\partial z} \left\{ \kappa_{\lambda}[T_L(z)] \frac{\partial T_L(z)}{\partial z} \right\} - [W_s^e(z)]$$

$$+ W_s^h(z)] + \frac{4\sigma}{\sqrt{\mathcal{S}}}[T_0^4 - T_{\mathrm{L}}^4(z)], \qquad (1)$$

where λ=TA (transverse-acoustic mode), LA (longitudinal-acoustic mode), TO (transverse-optical mode), and LO (longitudinal-optical mode), $\sigma = \pi^2 k_B^4/60\hbar^3 c^2$ is the Stefan-Boltzmann constant, T_0 is the constant surrounding temperature. Due to the z dependence of the lattice temperature $T_L(z)$, we employ a slab model in the z direction in this paper. With this model, the lattice temperature takes $T_L(z)$ in a narrow slab at z with a square cross-sectional area $\mathcal{S}$ and a thickness Δz. The initial condition of Eq. (1) is set by $T_L = T_i$ at $t=0$, where T_i is the initial thermal-equilibrium temperature between carriers and phonons. The boundary conditions of Eq. (1) are set by $\partial T_L(z)/\partial z = 0$ at the center $(z=0)$ of a symmetric quantum well and by $\Sigma_{\lambda}\kappa_{\lambda}[T_L(z)] \times [\partial T_L(z)/\partial z] = \sigma[T_0^4 - T_L^4(z)]$ at the two edges $(z = \pm z_{\max})$ of the square-shape sample. In this paper, we assume an electric-quantum limit for low carrier densities, i.e., the photoexcited electrons and holes only occupy the ground states of conduction and valence subbands. The unit volume specific heat of the semiconductor lattice introduced in Eq. (1) is[6]

$$c_V^{\lambda}[T_L(z)] = \left(\frac{\hbar^2}{4 k_B T_L^2(z)\mathcal{V}} \right) \sum_{\vec{q},q_z} \rho_{\lambda} \omega_{q,\lambda}^2(q_z) \sinh^{-2}\left(\frac{\hbar\omega_{q,\lambda}(q_z)}{2 k_B T_L(z)} \right),$$
$$(2)$$

where $\mathcal{V}$ is the volume of the sample, $\vec{Q} = (\vec{q}, q_z)$ is the three-dimensional wave vector of phonons, $\vec{q}$ is the two-dimensional wave vector in the xy plane of a quantum well, q_z is the phonon wave number in the z direction, $\rho_{LA} = \rho_{LO} = 1$, and $\rho_{TA} = \rho_{TO} = 2$. In addition, the unit-volume thermal conductivity introduced in Eq. (1) is given by

$$\kappa_{\lambda}[T_L(z)] = \frac{1}{3} s_{\lambda}^2 \tau_{ph} c_V^{\lambda}[T_L(z)], \qquad (3)$$

where τ_{ph} is the average phonon relaxation time, $s_{TA} = s_t$, $s_{LA} = s_{\ell}$, $s_{LO} = s_{TO} = 0$, and s_t and s_l are the sound velocities of TA and LA phonon modes, respectively. Moreover, the notation $\omega_{q,\lambda}(q_z)$ in Eq. (2) is the angular frequency of phonons. Using the Debye model for acoustic phonons,[27] we have $\omega_{q,TA}(q_z) = s_t\sqrt{q^2 + q_z^2}$ and $\omega_{q,LA}(q_z) = s_{\ell}\sqrt{q^2 + q_z^2}$. $\omega_{q,LO}(q_z) = \omega_{LO}$ is a constant from the Fröhlich coupling model,[28] and $\omega_{q,TO}(q_z) = \omega_{TO}$ is also considered to be a constant.

It has been known for a long time that the exciton effect at room temperature becomes negligible in GaAs quantum wells, as discussed at the beginning of this section. However, the interaction between electron and hole plasmas is still expected to play a major role during the second step of the four-step laser cooling model. The resulting detailed balance,[29] i.e., a steady-state condition for distributions of hot electrons and holes, between interacting electron and hole plasmas for individual energy states locks the carrier temperatures to a common value $T(z)$, which depends on the slab position. The strong confinement of the photoinduced carriers within quantum wells prevents carriers from diffusing in the z direction perpendicular to the quantum wells. The time that the carriers require to adjust their temperature is much shorter than the evolution time of the lattice temperature. Therefore, the conservation of the total energy of confined electrons and holes gives rise to the energy-balance equation[19] for the total energy of electrons and holes at each slab position during the last step of the four-step laser cooling model,

$$W_{ab}(z) - W_{sp}(z) + W_s^e(z) + W_s^h(z) = 0. \qquad (4)$$

Equation (4) can be used to adiabatically determine the spatial dependence of carrier temperature $T(z)$ for each profile of the lattice temperature $T_L(z)$ obtained from Eq. (1) at each moment. The carrier temperature will be thermally dragged down by the reduction of the lattice temperature with time.

The dominant source term in Eq. (1), $W_s^e(z) + W_s^h(z)$, is attributed to the inelastic scattering of photo-excited carriers with phonons during the second step of the four-step laser cooling model. The spatial distribution of the power exchanges $W_s^{\beta}(z)$ of electrons and holes with phonons are calculated to be[30]

$$W_s^{\beta}(z) = -\frac{8\pi}{\mathcal{S}}[\phi_1^{\beta}(z)]^2 \sum_{\vec{q},q_z,\lambda} \left\{ \int_{-\infty}^{+\infty} dz' \cos[q_z(z-z')] \right.$$

$$\left. \times [\phi_1^{\beta}(z')]^2 \right\} \times \omega_{q,\lambda}(q_z) |C_{q,\lambda}(q_z)|^2 \left[N_0\left(\frac{\hbar\omega_{q,\lambda}(q_z)}{k_B T_L(z)} \right) \right.$$

$$\left. - N_0\left(\frac{\hbar\omega_{q,\lambda}(q_z)}{k_B T(z)} \right) \right] \times \sum_{\vec{k}} (f_k^{\beta}[T(z)]$$

$$- f_{|\vec{k}+\vec{q}|}^{\beta}[T(z)]) \delta[E_{|\vec{k}+\vec{q}|}^{\beta} - E_k^{\beta} + \hbar\omega_{q,\lambda}(q_z)], \qquad (5)$$

where $\beta = e$, h for electrons (e) and holes (h), $\phi_1^{\beta}(z)$ represents the wave functions of the electrons and holes in their ground states. The free-carrier absorption, which is also called the phonon-assisted intraband photon absorption,[31] is neglected for weak pump fields, $\vec{k}$ is the two-dimensional wave vector of carriers in the xy plane of a quantum well, $E_k^{\beta} = \hbar^2 k^2 / 2m_{\beta}^*$ is the kinetic energy of carriers, m_{β}^* is the effective mass of carriers, and $N_0(x) = 1/[\exp(x) - 1]$ is the Bose-Einstein function. For λ=TA in Eq. (5), the coupling matrix is[32]

$$|C_{q,TA}(q_z)|^2 = \frac{2\hbar\sqrt{q^2 + q_z^2}}{2\rho_0 s_t \mathcal{V}} (eh_{14})^2 \frac{q^2(q^4 + 8q_z^4)}{4(q^2 + q_z^2)^4}, \qquad (6)$$

where ρ_0 is the mass density of ions and h_{14} is the piezoelectric potential of semiconductors. The screening effect from the carriers on the carrier-phonon interaction is neglected, as discussed at the beginning of this section. In addition, for λ=LA we have

$$|C_{q,LA}(q_z)|^2 = \frac{\hbar\sqrt{q^2+q_z^2}}{2\rho_0 s_\ell \mathcal{V}}\left(D^2 + (eh_{14})^2 \frac{9q^4 q_z^2}{2(q^2+q_z^2)^4}\right), \quad (7)$$

where D is the deformation-potential coefficient of semiconductors. For $\lambda = $ LO in Eq. (5), we use the Fröhlich coupling model[28] to get

$$|C_{q,LO}(q_z)|^2 = \frac{\hbar\omega_{LO}}{2\mathcal{V}}\left(\frac{1}{\epsilon_\infty} - \frac{1}{\epsilon_s}\right)\frac{e^2}{\epsilon_0(q^2+q_z^2)}, \quad (8)$$

where ϵ_∞ and ϵ_s are separately the high-frequency and static dielectric constants of semiconductors. However, the TO phonons do not directly couple to charged particles.

In Eq. (5), we have also introduced the dynamical distributions $f_k^\beta[T(z)]$ for photoinduced electrons ($\beta = e$) and holes ($\beta = h$), which changes with time through the time-dependent carrier temperature $T(z)$. During the second step of the four-step laser cooling model, quasiequilibrium Fermi-Dirac distributions for hot electrons and holes at the temperature $T(z)$ are assumed in this paper because the time for their ultrafast inelastic scattering with phonons (on the order of 1 ps) is much shorter than their radiative-decay time (on the order of 1 ns). This leads us to

$$f_k^\beta[T(z)] = \left[1 + \exp\left(\frac{E_1^\beta + \hbar^2 k^2/2m_\beta^* - \mu_\beta}{k_B T(z)}\right)\right]^{-1}, \quad (9)$$

where E_1^β represents the edge of the first subband of either electrons or holes, $\mu_\beta[T(z), n_{2D}]$ is the chemical potential of carriers, and n_{2D} is the sheet density of photoexcited carriers. The three-dimensional density function of the quantum well structure is given by $n_\beta(z) = n_{2D}|\phi_1^\beta(z)|^2$, which is uniform within the xy plane of the quantum well. For the second step, we further assume that the sheet density is constant during the adiabatic thermal drag of the carrier temperature by the lattice temperature, while the carrier distributions change from initially coherent ones to quasiequilibrium ones given by Eq. (9) through intraband scattering processes, including carrier-impurity, carrier-phonon, and carrier-carrier scattering. The carrier-phonon scattering is primarily responsible for the redistribution of kinetic energies of photoexcited carriers[33] into an initial thermal-equilibrium state just prior to the radiative lifetime (nanosecond) of the system with an initial equilibrium temperature T_i for both carriers and phonons. On the other hand, the carrier-impurity and carrier-carrier scatterings are responsible for the redistribution of the carrier momentum[33] into this thermal-equilibrium state. In addition, the carrier-carrier scattering guarantees a common temperature for electrons and holes.[29] Due to the z dependence of the carrier temperature $T(z)$, we employ a slab model. With this model, the carrier temperature is $T(z)$ within a narrow slab with a thickness Δz at z, and the chemical potential $\mu_\beta[T(z), n_{2D}]$ in each slab for fixed $T(z)$ and n_{2D} satisfies an equation for the the conservation of the number of created carriers,

$$\frac{1}{\pi}\int_0^{+\infty} k\,dk\left[1 + \exp\left(\frac{E_1^\beta + \hbar^2 k^2/2m_\beta^* - \mu_\beta[T(z), n_{2D}]}{k_B T(z)}\right)\right]^{-1}$$
$$- n_{2D} = 0, \quad (10)$$

where $\beta = e, h$, $\int|\phi_1^\beta(z)|^2\,dz = 1$, and $\int n_\beta(z)dz = n_{2D}$.

The laser cooling $[T_L(z) < T_i]$ or laser heating $[T_L(z) > T_i]$ at each position z depends on the negative or positive sign of the quantity $W_{ab}(z) - W_{sp}(z)$, since the dominant source term $-[W_s^e(z) + W_s^h(z)]$ in Eq. (1) equals $W_{ab}(z) - W_{sp}(z)$ by virtue of Eq. (4). During the third step of the four-step laser cooling model, the radiative decay and the weak optical absorption compete with each other. The former takes power away from the system, while the latter adds power to the system. The z-dependent power loss due to the escaping spontaneous photons is found to be[19,34]

$$W_{sp}(z) = \xi_{eh}(z)\frac{2\sqrt{\epsilon_r}e^2}{\pi\hbar^2 m_0 \epsilon_0 c^3 \mathcal{S}}\left(\frac{m_0}{m_e^*} - 1\right)\frac{E_G'(E_G' + \Delta_0)}{E_G' + 2\Delta_0/3}$$
$$\times\left(\int_{-\infty}^{\infty} dz'\,\xi_{eh}(z')\right) \times \sum_{\vec{k}}\left[E_G'\right.$$
$$\left. + \frac{\hbar^2 k^2}{2\mu^*}\right]^2 f_k^e[T(z)]f_k^h[T(z)], \quad (11)$$

where $\xi_{eh}(z) = \phi_1^e(z)\phi_1^h(z)$ represents the overlap of electron-hole wave functions, $E_G' = E_G + E_1^e + E_1^h$ is the bandgap of the quantum well, E_G is the bandgap of the bulk semiconductor for the layer forming the well, Δ_0 is the spin-orbit splitting, $1/\mu^* = 1/m_e^* + 1/m_h^*$ is the reduced mass of carriers, m_0 is the free-electron mass, and $\epsilon_r = (\epsilon_\infty + \epsilon_s)/2$ is the average dielectric constant of the semiconductor. The small temperature dependence of E_G is neglected for the limited variation of the lattice temperature that occurs. Here, we have also neglected nonradiative decay to defect states within the bandgap (proportional to the product of the trap density, N_t, and the carrier density) by assuming a relatively clean semiconductor binary crystal with $N_t \ll n_{2D}$, as well as the nonradiative decay due to Auger recombination[20] by assuming a very low carrier density. The escape probability of emitted photons is taken to be one for simplification. If included, the reabsorption of emitted photons would cause a slight decrease of the power loss in Eq. (11) and a slight increase of the power gain in Eq. (12) below at the same time. The z-dependent power gain due to the optical absorption of the laser field in the presence of carrier scattering is found to be[19]

$$W_{ab}(z) = \frac{8}{\hbar\mathcal{S}}\xi_{eh}(z)\left[\frac{e^2\mathcal{E}_p^2}{2m_0\Omega_p^2}\left(\frac{m_0}{m_e^*} - 1\right)\frac{E_G'(E_G' + \Delta_0)}{E_G' + 2\Delta_0/3}\right]$$
$$\times\left(\int_{-\infty}^{\infty} dz'\,\xi_{eh}(z')\right) \times \sum_{\vec{k}}\left(E_G' + \frac{\hbar^2 k^2}{2\mu^*}\right)$$
$$\times(1 - f_k^e[T(z)] - f_k^h[T(z)])$$
$$\times\frac{\gamma_0}{[E_G' + \hbar^2 k^2/2\mu^* - \hbar\Omega_p]^2 + \gamma_0^2}, \quad (12)$$

where γ_0 is the homogeneous level broadening due to the

finite lifetime of quasiparticles, $\mathcal{E}_p$ is the amplitude of the pump laser, and Ω_p is the angular frequency of the pump laser.

The sheet density n_{2D} of carriers generated by photoexcitation during the first step of the four-step laser cooling model is assumed constant during the adiabatic change of the carrier temperature. The relationship between n_{2D} and the pump field strength $\mathcal{E}_p$ for the initial time can be obtained from a coherent density-matrix theory[35] in the absence of carrier scattering during the first step. We emphasize that the carrier-photon system considered in this paper is not a blackbody system (rather, more like a grey-body system) and that the use of a blackbody assumption[36] cannot be justified. This is attributed to the lack of detailed thermal balance between input laser photons and induced carriers, to the different carrier and lattice temperatures, and to the change of carrier distributions with time during the cooling (or heating) process. The induced sheet density in Eq. (10) due to photoexcitation is calculated as[35]

$$n_{2D} = \frac{1}{2\pi} \int_0^{+\infty} k \, dk \left(1 - \frac{|E_G' - \hbar\Omega_p + \hbar^2 k^2/2\mu^*|}{\sqrt{(E_G' - \hbar\Omega_p + \hbar^2 k^2/2\mu^*)^2 + 4\Delta_R^2}} \right), \tag{13}$$

where the Rabi splitting $2\Delta_R$, which determines the power broadening in the coherent distribution of carriers under resonant excitation, is given by

$$\Delta_R^2 = \frac{e^2 \mathcal{E}_p^2}{2m_0 \Omega_p^2} \left(\frac{m_0}{m_e^*} - 1 \right) \frac{E_G'(E_G' + \Delta_0)}{E_G' + 2\Delta_0/3} \left(\int_{-\infty}^{\infty} dz \, \xi_{eh}(z) \right)^2. \tag{14}$$

On the other hand, the initial thermal-equilibrium temperature $T_i (T_i < T_0)$ for carriers and phonons is obtained from the energy conservation law

$$\sum_{\vec{q}, q_z, \lambda} \hbar\omega_{q,\lambda}(q_z) \left[N_0 \left(\frac{\hbar\omega_{q,\lambda}(q_z)}{k_B T_0} \right) - N_0 \left(\frac{\hbar\omega_{q,\lambda}(q_z)}{k_B T_i} \right) \right]$$
$$= 2 \sum_{\vec{k}, \beta} \frac{\hbar^2 k^2}{2m_\beta} \left[f_k^\beta [T_i] - \frac{1}{2} \left(1 - \frac{|E_G' - \hbar\Omega_p + \hbar^2 k^2/2\mu^*|}{\sqrt{(E_G' - \hbar\Omega_p + \hbar^2 k^2/2\mu^*)^2 + 4\Delta_R^2}} \right) \right], \tag{15}$$

where $\lambda = $ TA, LA, TO, LO, and $\beta = e, h$, respectively. For very low carrier densities, we expect $T_i \approx T_0$.

As stated at the beginning of this section, n_{2D} must be kept low to meet the criterion of laser cooling of undoped semiconductor quantum wells. Under this assumption, the ground-state electron and hole wave functions, $\phi_1^e(z)$ and $\phi_1^h(z)$, and corresponding subband edges, E_1^e and E_1^h, in the quantum well are simply found by solving the single-particle Schrödinger equation
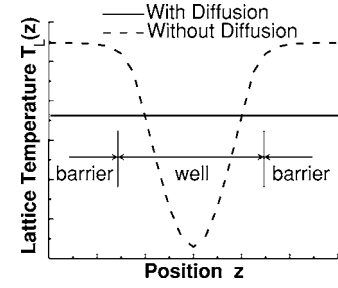

FIG. 2. An illustration of the spatial profiles of the lattice temperatures $T_L(z)$ as a function of the position z with (solid curve) and without (dashed curve) the phonon thermal diffusion after the photoluminescence in the well (surrounded by two barriers) starts. A V-shape feature (dashed curve) at the well center in the spatial profile of the lattice temperature can be seen. The phonon diffusion reduces the lattice temperature in the barrier and increases the lattice temperature inside the well at the same time. Finally, a uniform $T_L(z)$ is established by including the fast phonon-diffusion effect (solid curve). Although the lattice temperature becomes independent of z, the carrier temperature can still exhibit a V-shape feature at the well center due to the lack of the thermal diffusion of carriers in the z direction.

$$-\frac{\hbar^2}{2m_\beta^*} \frac{d^2}{dz^2} \phi_1^\beta(z) + V_{QW}^\beta(z) \phi_1^\beta(z) = E_1^\beta \phi_1^\beta(z), \tag{16}$$

where $\beta = e, h$, and $V_{QW}^e(z)$ and $V_{QW}^h(z)$ represent the conduction (V_c) and valence (V_p) band offsets, respectively.

III. NUMERICAL RESULTS AND DISCUSSIONS

In our numerical calculations, we have chosen GaAs as a material for the quantum well layer, and $Al_{0.3}Ga_{0.7}As$ as the material for the two barrier layers surrounding the quantum well. The parameters for this quantum well structure are as follows: $m_e^* = 0.067m_0$, $m_h^* = 0.62m_0$, $E_G = 1.424$ eV, $V_c = 243$ meV, $V_p = 131$ meV, $\Delta_0 = 0.341$ eV, $\epsilon_s = 13.18$, $\epsilon_\infty = 10.89$, $\epsilon_r = (\epsilon_s + \epsilon_\infty)/2$, $\hbar\omega_{LO} = 36.25$ meV, $\hbar\omega_{TO} = 33.29$ meV, $s_l = 5.14 \times 10^5$ cm/s, $s_t = 3.04 \times 10^5$ cm/s, $\rho_0 = 5.3$ g/cm^3, $D = -9.3$ eV, $h_{14} = 1.2 \times 10^7$ V/cm, and $\tau_{ph} = 3$ ps. The other parameters include $\hbar\Omega_p - E_G' = 9.8$ meV, $\mathcal{E}_p = 30$ V/cm, $\gamma_0 = 0.66$ meV, $\mathcal{S} = 1$ cm^2, and $T_i = T_0$. With the parameters given above, our calculation shows that $E_1^e = 83.6$ meV, $E_1^h = 17.0$ meV, and $E_G' = E_G + E_1^e + E_1^h = 1.524$ eV.

Figure 2 presents a qualitative illustration for the change of the spatial dependence of the lattice temperature $T_L(z)$ in the presence (solid curve) or the absence (dashed curve) of phonon thermal diffusion. When the thermal diffusion of phonons in Eq. (1) is not included, we find a V-shape feature (dashed curve) in $T_L(z)$ at the center of a quantum well surrounded by two barriers. However, this V-shape feature in $T_L(z)$ disappears (solid curve) after the thermal diffusion of phonons is included. The phonon diffusion reduces the lattice temperature in the barrier and increases the lattice temperature inside the well simultaneously. Finally, a uniform $T_L(z)$ will be established as a result of the phonon diffusion. We emphasize that the carrier temperature $T(z)$ is still expected
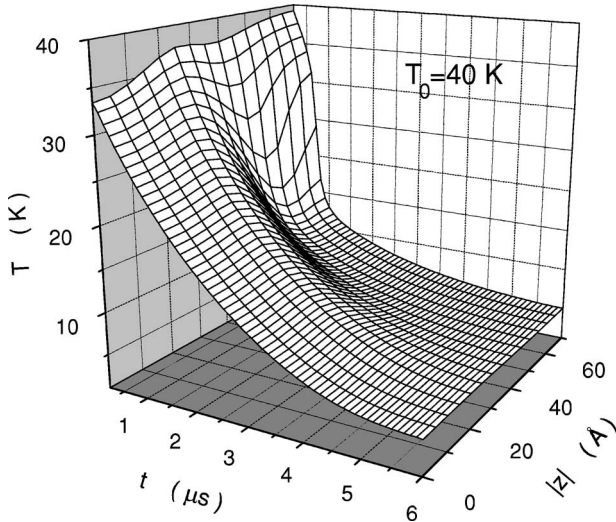
FIG. 3. 3D plot of the calculated carrier temperature T as functions of time t and position $|z|$ at $T_0=40$ K, where T is a symmetric function of z with respect to $z=0$, and $|z|=22.5$ Å represents two interfaces of the GaAs quantum well sandwiched by two $Al_{0.3}Ga_{0.7}As$ barrier layers. Here, the half-V-shape feature at $z=0$ in the spatial profile of the carrier temperature is clearly visible within a few radiative lifetimes (nanoseconds) after the pump is turned on, and it disappears after 6 μs from the start of the photoluminescence.

to exhibit a V-shape feature at the well center due to the lack of the thermal diffusion of carriers in the z direction although the lattice temperature $T_L(z)$ becomes independent of z. The value of $T_L(z)$ at two edges of the sample is expected to be lower than the surrounding temperature T_0 because of a positive large thermal conductivity $\kappa_\lambda[T_L(z)]$ and a positive non-zero derivative of $T_L(z)$ with respect to z in the boundary condition $\Sigma_\lambda \kappa_\lambda[T_L(z)][\partial T_L(z)/\partial z]=\sigma[T_0^4-T_L^4(z)]$ at $z=\pm z_{max}$.

Figure 3 displays the time evolution of the carrier-temperature profile $T(z)$ as a function of $|z|$ at $T_i=T_0=40$ K. Here, $T(z)$ is symmetric with respect to $z=0$. The interesting feature of $T(z)$, namely a half-V-shape feature and a lower value in comparison with T_0 at the edge of the sample due to $T_L<T_0$ there, appears within a few radiative lifetimes (nanoseconds) after the pump is turned on, and is a combined result of the restricted net power loss $W_{sp}(z)-W_{ab}(z)$ in Eq. (4) within the quantum well and the lack of thermal diffusion of carriers in the z direction. The carrier temperature $T(z)$ is adiabatically obtained from a given profile of the lattice temperature $T_L(z)$ at each moment. $T(z)$ is found to be thermally dragged down by $T_L(z)$ with time due to the strong carrier-phonon scattering that tightly locks $T(z)$ near and slightly below $T_L(z)$ (displayed and explained in detail by Figs. 6 and 7, later). It is evident from Fig. 3 that the carrier-temperature "V" profile is effectively suppressed while the carrier temperature is cooled down. In addition, the cooling rate dT/dt decreases with the carrier temperature. In this case, the inelastic phonon scattering of photo-excited carriers mainly comes from the LA and TA phonons at $T\lesssim40$ K. After 6 μs from the start of photoluminescence, the half-V-shape feature at $z=0$ has essentially vanished, as shown in Fig. 3. How-
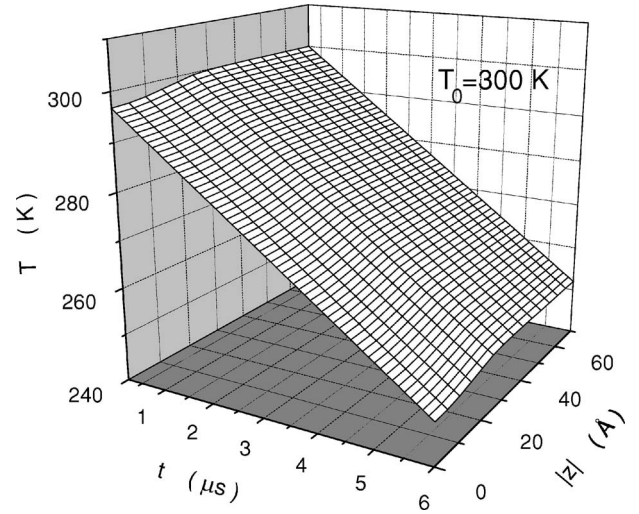

FIG. 4. 3D plot of the calculated carrier temperature T as functions of time t and position $|z|$ at $T_0=300$ K. Here, the visible half-V-shape feature at $z=0$ in the spatial profile of the carrier temperature is retained, even after 6 μs from the start of the photoluminescence.

ever, the situation in Fig. 4 is completely different at $T_0=300$ K. The carrier-temperature profile at $T_0=300$ K does not change at all as the carrier temperature decreases, and dT/dt is kept constant with time. The initial half-V-shape feature at $z=0$ remains constant throughout the time evolution of $T(z)$. For this range of the carrier temperatures, the inelastic phonon scattering of photoexcited carriers is very effective and dominated by the LO phonons.

Using Fig. 5, we may explain the difference between Figs. 3 and 4, where the time evolution of the net power-loss profile $W_{sp}(z)-W_{ab}(z)$ is presented at $T_0=40$ K. The z dependence in the ground-state wave function $\phi_1^\beta(z)$ for carriers, as determined by Eq. (16), is directly reflected by $\xi_{eh}(z)=\phi_1^e(z)\phi_1^h(z)$ in $W_{sp}(z)-W_{ab}(z)$, as seen from Eqs. (11) and (12). From Fig. 5 we find that the net power loss through the

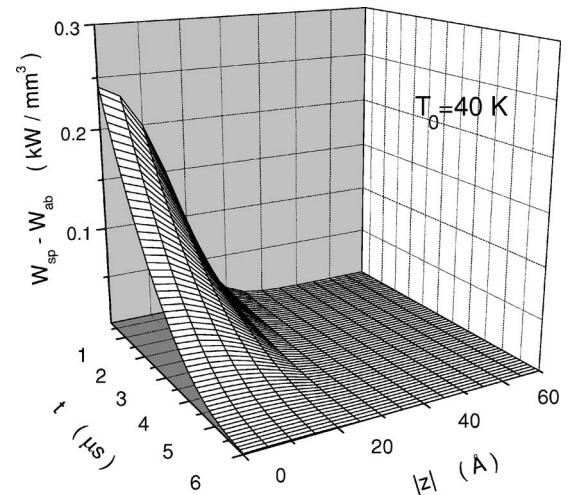FIG. 5. 3D plot of the calculated power-loss density $W_{sp}-W_{ab}$ as functions of time t and position $|z|$ at $T_0=40$ K, where $W_{sp}-W_{ab}$ is also a symmetric function of z with respect to $z=0$.
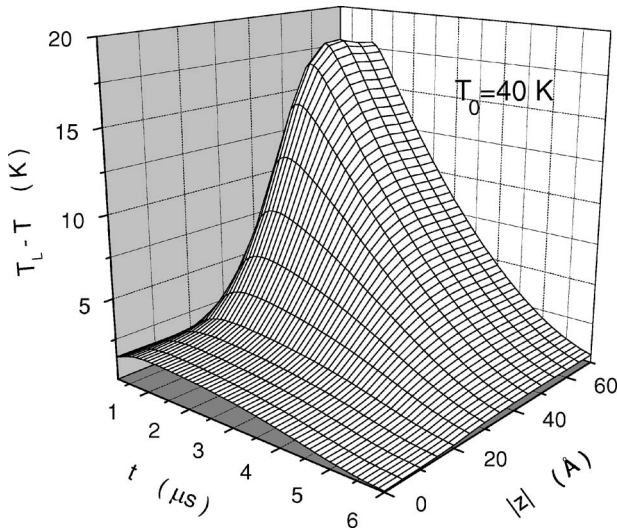
FIG. 6. 3D plot of the calculated difference between the lattice and carrier temperatures $T_L - T$ as functions of time t and position $|z|$ at $T_0 = 40$ K, where $T_L - T$ is a symmetric function of z with respect to $z = 0$.

inelastic scattering of two-dimensional carriers with three-dimensional LA and TA phonons is maximized at the well center $z = 0$, but the inelastic scattering is nearly zero in the barrier regions ($|z| > 22.5$ Å) due to the lack of available carriers there. However, the initial net power-loss profile $W_{sp}(z) - W_{ab}(z)$ disappears when $t = 6$ μs because of the nearly unchanging power gain W_{ab} due to $1 - f_k^e[T(z)]$ $- f_k^h[T(z)] \approx 1$ in Eq. (11), as well as the strong simultaneous reduction of power loss W_{sp} due to the strong reduction of $f_k^e[T(z)] f_k^h[T(z)]$ with $T(z)$ in Eq. (12), while the carrier temperature cools down. The features seen in this figure for the time evolution of the net power-loss profile $W_{sp}(z) - W_{ab}(z)$ directly provide an explanation to the complete suppression of the carrier-temperature "V" profile $T(z)$ at $T_0 = 40$ K in Fig. 3 when $t = 6$ μs.

The strong carrier-phonon inelastic scattering in GaAs is dominated by LO phonons at room temperature in GaAs. On the other hand, the carrier-phonon scattering will be weak and dominated by LA and TA phonons if the lattice temperature T_L is kept low, e.g. $T_L = 40$ K. The carrier-phonon coupling strength dynamically determines the magnitude of the difference $T_L(z) - T(z)$ between the lattice and carrier temperatures through the energy-balance equation in Eq. (4) for a given lattice temperature $T_L(z)$. For the case of laser cooling with $dT/dt < 0$ or a positive net power loss $W_{sp}(z) - W_{ab}(z) > 0$, we find $T_L - T > 0$, i.e., the carriers gain thermal energy from the lattice. In this case, the carrier temperature $T(z)$ is dragged down by the reduction of the lattice temperature $T_L(z)$ with time, i.e., the thermal-drag effect. The thermal-energy exchange between carriers and phonons is characterized by the z-dependent exchange specific-heat $c_{ex}(z)$ (in unit volume and time) defined by the relation $c_{ex}(z)[T_L(z) - T(z)] = W_s^e(z) + W_s^h(z)$. We display in Fig. 6 the time evolution of the profile for the difference $T_L - T$ between the lattice and carrier temperatures at $T_0 = 40$ K. From Fig. 6 we find that the initial difference profile $T_L(z) - T(z)$ is seen
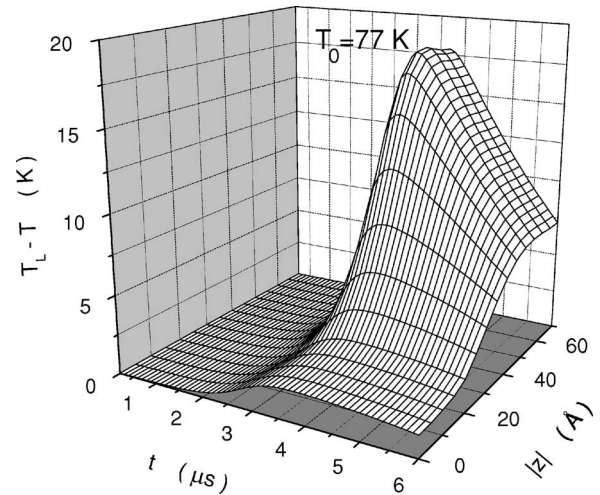

FIG. 7. 3D plot of the calculated difference between the lattice and carrier temperatures $T_L - T$ as functions of time t and position $|z|$ at $T_0 = 77$ K.

to be larger in the barrier regions than in the well region. This is attributed to the reduction of the carrier-phonon coupling strength, or a small value of $c_{ex}(z)$, in the barrier region due to the lack of available carriers there. The initial difference profile at $T_0 = 40$ K nearly disappears when $t = 6$ μs due to the suppressed net power loss by the reduced carrier temperature $T(z)$, as shown in Fig. 5. However, the situation in Fig. 7 with $T_0 = 77$ K is dramatically different. We do not see an initial enhancement of $T_L - T$ in the barrier region for this initial temperature because of the relatively strong carrier-phonon coupling strength, or a large value of $c_{ex}(z)$, with LO phonons at $T_0 = 77$ K. As the lattice temperature is cooled down to 40 K at $t = 6$ μs, the strong coupling with LO phonons at 77 K is replaced by a weak coupling with LA and TA phonons at 40 K. The suppression of $c_{ex}(z)$ with the reduced lattice temperature leads to an enhancement of $T_L - T$ in the barrier region in Fig. 7 at $t = 6$ μs. The enhancement of $T_L - T$ in the barrier region will further evolve with time, as described in Fig. 6.

IV. CONCLUSIONS

In conclusion, a successive four-step model has been proposed for spatially selective laser cooling of carriers in an undoped AlGaAs/GaAs/AlGaAs quantum well. Based on this model, a thermal-diffusion equation for phonons, including carrier-phonon inelastic scattering and thermal radiation from the surrounding environment as source terms, has been derived. At the same time, an energy-balance equation for the total energy of hot electrons and holes at each position has been established. These two equations have been applied together to find the time evolution of the lattice temperature, and to adiabatically find the spatial dependence of the carrier temperature for a given lattice temperature at each moment.

In addition, two features in the carrier temperature have been predicted; there is a V-shape feature at the well center and a lower value in comparison with the surrounding temperature. The former is attributed to the fact that the net

power loss only effectively occurs within the well region and is maximized at the well center, while the latter is attributed to the fact that there exists a positive large thermal conductivity and a positive nonzero derivative of the lattice temperature at the boundaries of two edges of the sample. These features also agree with our intuitive expectations from spatially selective laser cooling of carriers in an undoped quantum well. The really interesting finding in this paper is that the V-shape feature in the carrier temperature survives only when the initial lattice temperature is above 150 K. A lower initial lattice temperature implies a lower ultimate lattice temperature after a time of lattice cooling. This interesting finding is explained by the fact that the fluorescence of the system greatly decreases when the carrier temperature is thermally dragged down from its initial temperature due to carrier-phonon coupling to a value below 150 K, which suppresses the net power loss of the system. Another really interesting finding in this paper is that the difference between the lattice and carrier temperatures is larger in the barrier regions than in the well region. A smaller carrier-phonon coupling strength implies a larger difference between the lattice and carrier temperatures. The mechanism for laser cooling of the carrier temperature that is pinned to and slightly lower than the lattice temperature is built on the thermal-drag effect. At 40 K or below, the carrier-phonon coupling strength is much smaller in the barrier regions compared to that in the well region due to the lack of available carriers in the barriers.

[1] B. F. Levine, J. Appl. Phys. **74**, R1 (1993).

[2] H. L. Edwards, Q. Niu, G. A. Georgakis, and A. L. de Lozanne, Phys. Rev. B **52**, 5714 (1995).

[3] G. D. Mahan, J. O. Sofo, and M. Martkowiak, J. Appl. Phys. **83**, 4683 (1998).

[4] J. Pekola, R. Schoelkopf, and J. Ullom, Phys. Today **41**, 41 (2004).

[5] A. G. Mal'shukov and K. A. Chao, Phys. Rev. Lett. **86**, 5570 (2001).

[6] J. M. Ziman, *Principles of the Theory of Solids*, 1st ed. (Cambridge University Press, Cambridge, 1964).

[7] R. I. Epstein, M. I. Buchwald, B. C. Edwards, T. R. Gosnell, and C. E. Mungan, Nature **37**, 500 (1995).

[8] P. Pringsheim, Z. Phys. **57**, 739 (1929).

[9] L. Landau, J. Phys. (Moscow) **10**, 503 (1946).

[10] H. Gauck, T. H. Gfroerer, M. J. Renn, E. A. Cornell, and K. A. Bertness, Appl. Phys. A **64**, 143 (1997).

[11] G. Lei, J. E. Anderson, M. I. Buchwald, B. C. Edwards, R. I. Epstein, M. T. Murtagh, and G. H. Sigel, Jr., IEEE J. Quantum Electron. **34**, 1839 (1998).

[12] B. C. Edwards, J. E. Anderson, R. I. Epstein, G. L. Mills, and A. J. Mord, J. Appl. Phys. **86**, 6489 (1999).

[13] J. Fernandez, A. Mendioroz, A. J. Garca, R. Balda, and J. L. Adam, Phys. Rev. B **62**, 3213 (2000).

[14] C. E. Mungan, J. Opt. Soc. Am. B **20**, 1075 (2003).

[15] J. L. Clark and G. Rumbles, Phys. Rev. Lett. **76**, 2037 (1996).

[16] C. W. Hoyt, M. Sheik-Bahae, R. I. Epstein, B. C. Edwards, and J. E. Anderson, Phys. Rev. Lett. **85**, 3600 (2000).

[17] A. N. Oraevsky, J. Russ. Laser Res. **17**, 471 (1996).

[18] L. A. Rivlin and A. A. Zadernovsky, Opt. Commun. **139**, 219 (1997).

[19] D. Huang, T. Apostolova, P. M. Alsing, and D. A. Cardimona, Phys. Rev. B **70**, 033203 (2004).

[20] M. Sheik-Bahae and R. I. Epstein, Phys. Rev. Lett. **92**, 247403 (2004).

[21] T. Apostolova, D. Huang, P. M. Alsing, and D. A. Cardimona, Phys. Rev. A **71**, 013810 (2005).

[22] We have reported preliminary results of the theoretical model in this paper at a *QWIP workshop* meeting in Canada.

[23] G. Bastard, *Wave Mechanics Applied to Semiconductor Heterostructures* (J. Wiley, New York, 1988), pp. 31–62.

[24] S. Das Sarma, R. Jalabert, and S.-R. Eric Yang, Phys. Rev. B **41**, 8288 (1990).

[25] G. D. Mahan, Phys. Rev. **163**, 612 (1967); G. D. Mahan, *Many-Particle Physics* (Plenum, New York, 1981), pp. 725–742.

[26] A. C. Tselis and J. J. Quinn, Phys. Rev. B **29**, 3318 (1984).

[27] C. Kittel, *Introduction to Solid State Physics*, 2nd ed. (J. Wiley, New York, London, 1956), pp. 118–156.

[28] H. Fröhlich and B. V. Paranjape, Proc. Phys. Soc. London, Sect. B **69**, 21 (1956).

[29] J. Li and C. Z. Ning, Phys. Rev. A **66**, 023802 (2002).

[30] X. L. Lei and C. S. Ting, Phys. Rev. B **32**, 1112 (1985).

[31] D. Huang, T. Apostolova, P. M. Alsing, and D. A. Cardimona, Phys. Rev. B **69**, 075214 (2004).

[32] S. K. Lyo and D. Huang, Phys. Rev. B **66**, 155307 (2002).

[33] M. Lindberg and S. W. Koch, Phys. Rev. B **38**, 3342 (1988).

[34] D. Huang and S. K. Lyo, Phys. Rev. B **59**, 7600 (1999).

[35] S. Schmitt-Rink, D. S. Chemla, and H. Haug, Phys. Rev. B **37**, 941 (1988).

[36] H. Haug and S. Schmitt-Rink, J. Opt. Soc. Am. B **2**, 1135 (1985).